Automatic Segmentation of Fluid-Associated Abnormalities and Pigment Epithelial Detachment in Retinal SD-OCT Images

Qiang CHEN, Zexuan JI, Tao WANG, Yuzhu TAND, Chenchen YU, Okuwobi Idowu PAUL and Loza Bekalo SAPPA

Nanjing University of Science & Technology
chen2qiang@njust.edu.cn

Abstract. ***Objective:*** Accurate segmentation of fluid-associated abnormalities and pigment epithelial detachment (PED) in spectral domain optical coherence tomography (SD-OCT) is vital for the assessment of retinal diseases. A novel deep learning based segmentation algorithm was proposed to achieve this aim. ***Methods:*** In the first stage, intraretinal fluid (IRF) was segmented using faster R-CNN. In the second stage, in order to segment subretinal fluid (SRF), voxels detected by faster R-CNN are regarded as seeds to perform 3D region growing. In the third stage, an effective RPE layer segmentation is helpful for us to locate PED. ***Results:*** Experimental results from three types of SD-OCT volumes, including Cirrus, Spectralis and Topcon, with fluid-associated abnormalities and PED, demonstrate that our method can almost achieve a overlapping ratio of 60%, respectively, for lesion regions. ***Conclusion:*** We report a fully automatic method for the segmentation of fluid-associated abnormalities and PED, which shows the potential to improve clinical therapy for retinal lesion.

Keywords: fluid-associated abnormalities, pigment epithelial detachment, segmentation, faster R-CNN, region growing.

1 Introduction

Spectral domain optical coherence tomography (SD-OCT) has become an indispensable imaging modality for the diagnosis and treatment of retinal diseases as it can non-invasively produce high-resolution cross-sectional images. The 3D volumetric OCT scan can accurately depict cross-sectional features of detached retina structure change and provide detailed anatomic assessments [1].

Fluid-associated abnormalities includes two types: intraretinal fluid (IRF) and subretinal fluid (SRF). In a macular centered B-scan, fluid-associated abnormalities regions appear as well-circumscribed hyporeflexia areas [3], among IRF regions locate between the internal limiting membrane (ILM) and the inner/outer segment (IS/OS) junction (Fig. 1(a)), and SRF regions locate between IS/OS junction and retinal pigment epithelium (RPE) (Fig. 1(b)). Pigment epithelial detachment (PED) is a prominent feature of many chorioretinal disease processes, including AMD, polypoidal

choroidal vasculopathy, central serous chorioretinopathy, and uveitis. PED can be classified as serous, fibrovascular, or drusenoid, which is associated with sub-RPE fluid and RPE deformation (Fig. 1(c)) [3]. IRF, SRF and PED may appear at the same eyes (Fig. 1(d)).

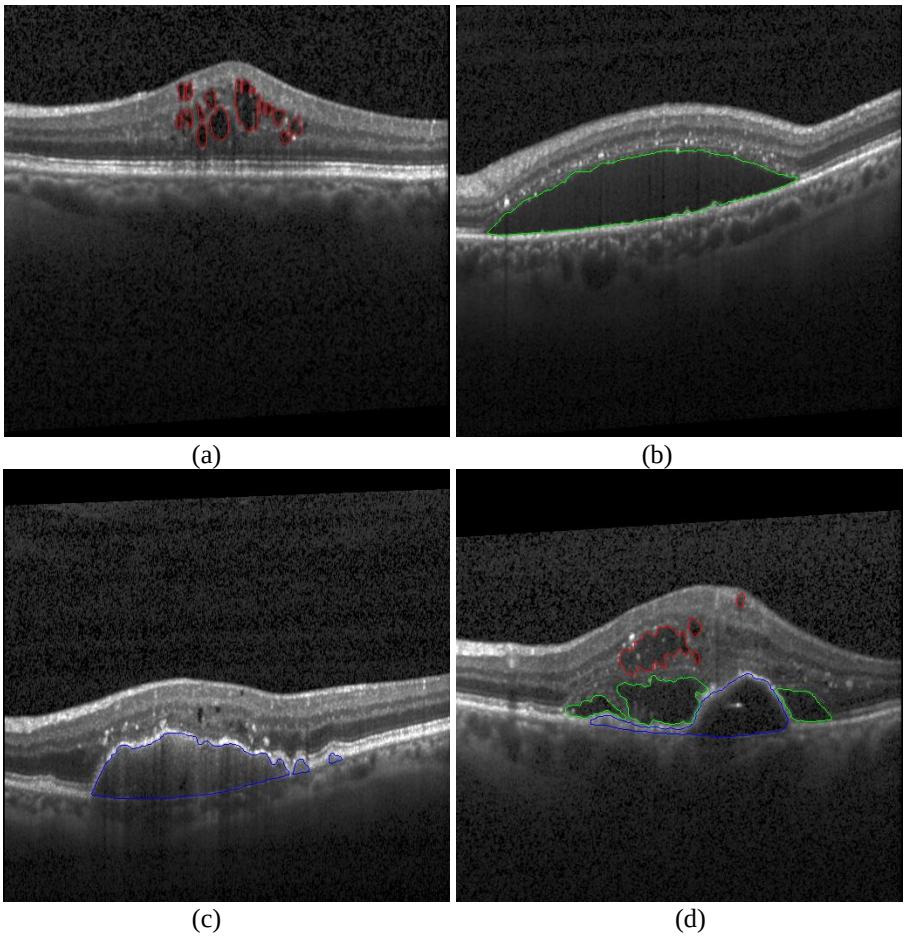

Fig. 1. OCT image of IRF, SRF and PED. Red region indicates IRF, green region indicates SRF, and blue region indicates PED. (a) OCT image of eyes suffering from IRF. (b) OCT image of eyes suffering from SRF. (c) OCT image of eyes suffering from PED. (d) OCT image of eyes suffering from IRF, SRF and PED meanwhile.

In these cases, segmentation of fluid-associated abnormalities and PED becomes challenging due to the following four reasons. First, the degradation of image quality caused by abnormalities may affect the segmentation performance and OCT images from different equipment could reduce the versatility of the algorithm. Second, retinal diseases could destroy the inherent structure of each layer, consequently have a strong impact on layer segmentation. Third, the appearance, texture, volume, location of

lesion region vary greatly. Four, different diseases interfere with each other, which greatly increases the difficulty of segmentation. Therefore, new methods that can segment lesion region, including fluid-associated abnormalities and PED, are needed for quantitative analysis of these diseases.

To segment lesion region, some unsupervised segmentation methods have been proposed. Most of such methods are based on the grayscale and morphologic features of the retinal lesion regions in OCT scans, such as thresholding based approaches [4], fuzzy level sets with cross-sectional voting [5], locally-adaptive loosely-coupled level sets [6] etc. Additionally, a graph-search model was popular in medical image processing field to simultaneously segment the retinal layer and fluid-associated abnormalities [7]. Machine learning methods belong to supervised segmentation methods, which treat retinal lesion region segmentation as a binary classification problem based on the layer detection results. With the layer-dependent feature selection, various classifiers have demonstrated good results in identifying the lesion region from the background [8-10]. However, the performance of machine learning methods relies on the number of available training samples and incurs additional training costs.

In this paper, we present a novel method which contains faster R-CNN, region growing and effective layer segmentation for the segmentation of fluid-associated abnormalities and PED. In the first stage, intraretinal fluid (IRF) was segmented using faster R-CNN. In the second stage, in order to segment subretinal fluid (SRF), voxels detected by faster R-CNN are regarded as seeds to perform 3D region growing. In the third stage, an effective RPE layer segmentation is helpful for us to locate PED.

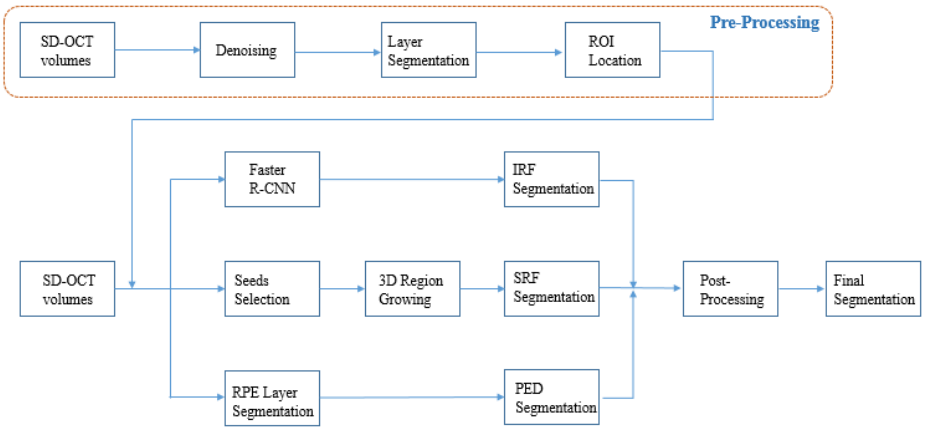

Fig. 2. Overview of the proposed framework

2 Methodology

Fig. 2 illustrates the overview of our framework. The ROI location phase aims to impose constraints on the search area using an automatic layer segmentation algorithm. Different strategies are utilized to segment different lesion region in corresponding ROI. Finally, we can obtain final segmentation after post-processing.

2.1 Pre-processing

There are a lot of speckle noise in retinal SD-OCT images due to OCT equipment adopts coherent beam reflection technique to detect living tissue. Such noise will reduce the quality of the image, even make computers be hard to recognize subtle structure or low-contrast features. In this paper, in order to improving the quality of the image, bilateral filter is used to remove speckle noise.

Effective layer segmentation is very necessary to limit search range. In retinal images, in general, some lesions only appear between specific layers, such as IRF appears between ILM and IS\OS, SRF appears between IS\OS and RPE, and PED appears between RPE and BM. Thus, after layer segmentation, we can set different ROI for different lesion region segmentation, this can greatly prevent the interference of other diseases, thereby increasing the precision of lesion region segmentation.

2.2 Faster R-CNN for IRF segmentation

Faster R-CNN is a unified, deep-learning-based real-time object detection method in computer vision [11].By sharing convolutional features with the down-stream detection network, the region proposal step is nearly cost-free. The learned RPN also improves region proposal quality and thus the overall object detection accuracy.

In this section, we will introduce the faster R-CNN for the IRF segmentation. IRF lesion region is regarded as the object that need to be detected. In training, we construct a smallest rectangular box that be able to include the IRF region. Then, we input training data, labels, and rectangular boxes to the faster R-CNN. After training, if we input a test retinal OCT B-scan to the network, the network would search the possible IRF region in the ROI obtained by effective layer segmentation and label the possible lesion area with rectangular box. Every rectangular box has a score from faster R-CNN. Finally, by a threshold, we can confirm the IRF lesion region which score is greater than the threshold.

2.3 3D region growing for SRF segmentation

We apply 3D region growing to segment the SRF area. Due to SRF is very close to PED, the interference of PED will decrease the accuracy of SRF segmentation using the faster R-CNN directly. In the first step of 3D region growing, two stable and reliable seeds should be selected. In order to obtain such seeds, we first utilize faster R-CNN to generate the initial seeds candidate set. Then clustering these seeds candidate into two classes by k-means. The center of clustering from two classes are regarded as the seeds. In the second step, we compute the mean value and variance of 26 points around the seeds in 3D space. The criterion of 3D region growing is shown as (1)

$$|I-avg| < sig \tag{1}$$

where I is the voxel need to be judged, avg is the mean value of 26 points around the seeds in 3D space, and sig is the variance of 26 points around the seeds in 3D

space. Similarly, layer segmentation is used to limit the search region in y-axis and a depth projection image is used to limit the search region in x-axis.

2.4 RPE layer segmentation for PED segmentation

An effective automatic layer segmentation not only limit the search region for the segmentation of IRF and SRF, but also be able to segment some specific lesion region. PED will result in the arching of RPE, so we can segment the PED area directly by computing the thickness of RPE and BM after layer segmentation.

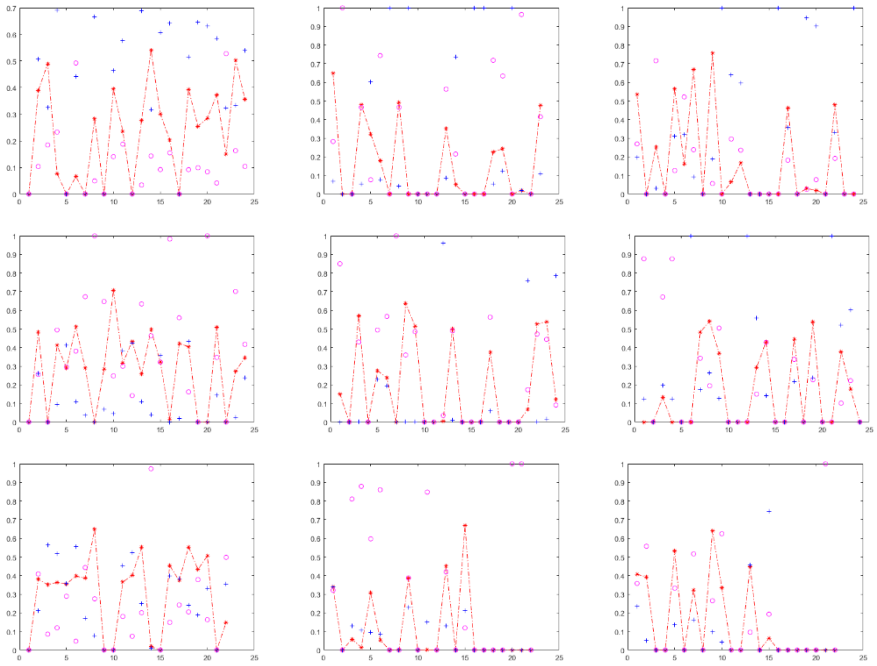

Fig. 3. The quantitative segmentation result, red dotted line indicates overlapping ratio, purple circle indicates the under-segmentation rate and blue plus sign indicates over-segmentation rate. First row shows the IRF, SRF, and PED's segmentation result of Cirrus. Second row shows the IRF, SRF, and PED's segmentation result of Spectralis. Third row shows the IRF, SRF, and PED's segmentation result of Topcon.

3 Experiment

The experiments are performed in three types of retinal SD-OCT volumes from different equipment, respectively are Cirrus, Spectralis, and Topcon. The experimental platform is MATLAB. The result will be estimated in both quantitative and qualitative.

Fig. 3 shows the qualitative estimation result, among red dotted line indicates overlapping ratio, purple circle indicates the under-segmentation rate and blue plus sign indicates over-segmentation rate. From the line chart, overlapping ratio, under-segmentation rate and over-segmentation rate are set to 0 if there are no such diseases in OCT volumes and we also succeed in that the lesion area was not detected. If we detect such lesion area that doesn't actually exist in OCT volume, the over-segmentation rate is set to 1. If we fail to detect such lesion area that actually exist in OCT volume, the under-segmentation rate is set to 1. The highest overlapping ratio for three types lesion areas are close to 0.7. The reason is that it is hard to detect lesion area which boundary is not obvious and area is very small.

Table 1 present Dice value, absolute volume difference (AVD), and region detection rate (RDR) of segmentation result. RDR indicates the probability that we detect lesion region, where each connected region represents a piece of lesion region. From the table, we can see that IRF could achieve the highest detection rate than other two diseases, because SRF and PED would interfere with each other seriously.

Table 1. Qualitative estimation result. Estimate Dice value, absolute volume difference (AVD), and region detection rate (RDR).

result		Dice (%)	AVD (voxel)	RDR (%)
Cirrus	IRF	0.9937	3.1117e+05	0.7585
	SRF	0.9967	1.7236e+05	0.5411
	PED	0.9961	1.7160e+05	0.7805
Spectralis	IRF	0.9951	2.4177e+05	0.6665
	SRF	0.9958	4.2477e+05	0.6497
	PED	0.9970	1.7273e+05	0.7558
Topcon	IRF	0.9980	5.5227e+05	0.6881
	SRF	0.9993	1.2409e+05	0.5742
	PED	0.9970	9.1565e+04	0.5730

4 Conclusion

There are no doubts that the difficulty of the segmentation will grow tremendously while there are a mixture of diseases. It is hard for us to segment all kinds of diseases using a generic method. Thus we design different segmentation method for different diseases. A faster R-CNN based method is used for the segmentation of IRF, a 3D region growing based method is used for the segmentation of SRF, and a RPE layer segmentation based method is used for the segmentation of PED. Three methods achieve goodish results. In future, we hope that the accuracy of segmentation will increase by combining more other effective methods and performing more effective experiment.

5 Reference

1. M. Wu et al. Automatic Subretinal Fluid Segmentation of Retinal SD-OCT Images with Neurosensory Retinal Detachment Guided by Enface Fundus Imaging. IEEE Transcations On Biomedical Engineering, pp.1-10, 2017.
2. L. Kiang et al. Formation of an Intraretinal Fluid Barrier in Cavitary Optic Disc Maculopathy. American Journal of Ophthalmology, vol.173, pp.34-44, 2017.
3. F. Shi et al. Automated 3-D Retinal Layer Segmentation of Macular Optical Coherence Tomography Images With Serous Pigment Epithelial Detachments. IEEE Transactions on Medical Imaging, vol.34, pp.441-452, 2015.
4. J. Yu et al. Study of subretinal exudation and consequent changes in acute central serous chorioretinopathy by optical coherence tomography. Am. J. Ophthalmol., vol.158, no.4, pp.752–756, 2014.
5. J. Wang et al. Automated volumetric segmentation of retinal fluid on optical coherence tomography. Biomed. Opt. Express, vol.7, no.4, pp.1577–1589, 2016.
6. J. Novosel et al. Locally-adaptive loosely-coupled level sets for retinal layer and fluid segmentation in subjects with central serous retinopathy. In IEEE Int. Symp. on Biomed. Imag. pp.702–705, 2016.
7. K. Li et al. Optimal surface segmentation in volumetric imagesa graph-theoretic approach. IEEE Trans. Pattern Anal. Mach. Intell., vol.28, no.1, pp.119–134, 2006.
8. X. Xu et al. Stratified sampling voxel classification for segmentation of intraretinal and subretinal fluid in longitudinal clinical oct data. IEEE Trans. Med. Imaging, vol.34, no.7, pp.1616–1623, 2015.
9. G. Quellec et al. Three-dimensional analysis of retinal layer texture: identification of fluid-filled regions in sd-oct of the macula. IEEE Trans. Med. Imaging, vol.29, no.6, pp.1321–1330, 2010.
10. A. Lang et al. Automatic segmentation of microcystic macular edema in oct. Biomed. Opt. Express, vol.6, no.1, pp.155–169, 2015.
11. S. Ren et al. Faster R-CNN: Towards Real-Time Object Detection with Region Proposal Networks. IEEE Transactions on Pattern Analysis & Machine Intelligence, vol.39, no.6, pp.1137–1146, 2017.